Electron acceleration by a self-diverging intense laser pulse

K. P. Singh,[1,*] D. N. Gupta,[1] V. K. Tripathi,[1] and V. L. Gupta[2]
[1]*Department of Physics, Indian Institute of Technology, New Delhi-110016, India*
[2]*Department of Electronic Science, University of Delhi, New Delhi-110021, India*
(Received 23 October 2003; published 28 April 2004)

Electron acceleration by a laser pulse having a Gaussian radial and temporal profile of intensity has been studied. The interaction region is vacuum followed by a gas. The starting point of the gas region has been chosen around the point at which the peak of the pulse interacts with the electron. The tunnel ionization of the gas causes a defocusing of the laser pulse and the electron experiences the action of a ponderomotive deceleration at the trailing part of the pulse with a lower intensity rather than an acceleration at the rising part of the laser pulse with a high intensity, and thus gains net energy. The initial density of the neutral gas atoms should be high enough to properly defocus the pulse; otherwise the electron experiences some deceleration during the trailing part of the pulse and the net energy gain is reduced. The rate of tunnel ionization increases with the increase in the laser intensity and the initial density of neutral gas atoms, and with the decreases in the laser spot size, which causes more defocusing of the laser pulse. The required initial density of neutral gas atoms decreases with the increase in the laser intensity and also with the decrease in the laser spot size.

DOI: 10.1103/PhysRevE.69.046406 PACS number(s): 52.38.Kd

I. INTRODUCTION

When a high power laser interacts with a gas at very high intensities, the electron's motion in the electric field of the laser becomes relativistic and MeV electrons are observed [1,2]. The onset of this regime is around $I\lambda^2 = 1.3 \times 10^{18}$ W/cm^2 μm^2, where I and λ are laser intensity and wavelength in units of W/cm^2 and μm, respectively, where the average kinetic energy of the electron oscillating in the laser field becomes equivalent to the rest mass energy. During recent years table-top high-peak power lasers with light intensities as high as $I\lambda^2 \cong 10^{21}$ W/cm^2 have been successfully developed [3]. This has led to the development of laser driven electron accelerators [4,5]. The early schemes envisaged the production of a large amplitude plasma wave in different accelerator schemes such as the plasma wake-field accelerator [6], the plasma beatwave accelerator [7], the laser wakefield accelerator (LWFA) [7,8], the resonant laser plasma accelerator [9], and the self-modulated laser wakefield accelerator (SMLWFA) [10–12].

Direct laser electron acceleration has received attention in recent years. An intense laser pulse ionizes the electrons from tightly bound atomic states. The energy gained by these electrons depends upon the pressure of the gas, the polarization of the laser pulse, the laser intensity, and the angular ejection angle [13,14]. Soldatov [15] found a distribution function of relativistic electrons produced by the tunnel ionization of a gas by an intense electromagnetic wave. It is well known that a planar laser pulse cannot be used for electron acceleration, since when it overtakes an electron the latter is ponderomotively driven forward in the rising part, but then backward in the trailing part, resulting in no net energy gain by the electron. However, if the propagating laser pulse is abruptly stopped at the solid target surface, the highly energetic electrons continue to move forward inertially and escape from the pulse as well as target without much loss in the energy, if their stopping distance is much larger than the laser skin depth and the target thickness, respectively [16]. In the interaction of high intensity laser pulses with underdense plasmas, relativistic filamentation causes a laser-beam breakup and a scattering of the beam, which results in a decrease in the intensity of the laser pulse [17]. The electrons leaving the pulse experience the action of a ponderomotive deceleration at the trailing part of the pulse with a lower intensity rather than an acceleration at the rising part of the laser pulse with a high intensity, and thus gain net energy. Similarly, an electron can gain net energy if it interacts with a laser pulse in vacuum during the rising part and in a gas during the trailing part of the pulse. A high-intensity laser pulse with an oscillating electric field comparable to the atomic field can ionize gases to form plasma by tunnel ionization [18–21]. A laser pulse with a Gaussian radial profile produces a plasma density maximum on the axis, causing the laser pulse to defocus due to the minimum of refractive index on the axis. This defocusing, in turn, weakens the laser intensity, reducing the ionization rate. The laser intensity interacting with the electron is higher during the rising part than that during the trailing part; therefore, the electron gains net energy. The energy retained by the electron depends upon the defocusing of the laser pulse, which in turn depends upon the laser spot size, the laser intensity, and the initial density of the neutral gas atoms. In this paper we find out how these factors affect electron acceleration.

This paper is organized as follows: The equations governing defocusing of the laser pulse and electron acceleration are formulated in Sec. II. Numerical results are presented in Sec. III. Finally, a brief discussion of the results is given in Sec. IV.

II. GOVERNING EQUATIONS

A schematic of electron acceleration by a short intense laser pulse in vacuum followed by a gas is shown in the

*Electronic address: k_psingh@yahoo.com

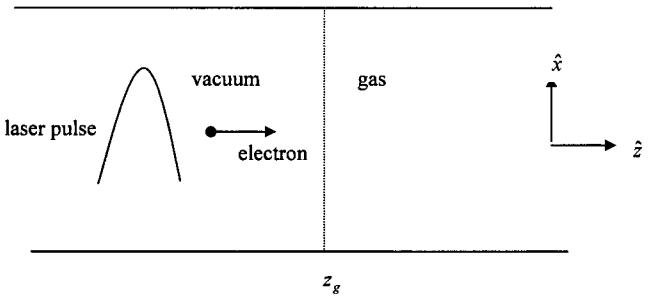

FIG. 1. Schematic of electron acceleration by a short intense laser pulse in vacuum followed by a gas.

Fig. 1. An electron interacts with a laser pulse in vacuum during the rising part and then in a gas during the trailing part. The laser pulse is defocused via tunnel ionization. Let us assume that gas starts at $z=z_g$.

At the entrance into the gas, $z=z_g$, the plane polarized laser field is

$$\mathbf{E} = \hat{x}E_0 \exp(-r^2/2r_0^2)\cos(\omega t - \omega z_g/c) \times \exp[-(t-(z_g-z_L)/v_g)^2/\tau_L^2], \quad (1)$$

where z_L is the initial position of the pulse peak and τ_L is its duration.

The tunnel ionization of the gas gives rise to a changing plasma density ω_p,

$$\frac{\partial \omega_p^2}{\partial t} = R(\omega_{pm}^2 - \omega_p^2), \quad (2)$$

where

$$R = \left(\frac{\pi|\mathbf{E}|}{2E_A}\right)^{1/2} \frac{I_0}{\hbar} \exp(-E_A/|\mathbf{E}|) \quad (3)$$

is the rate of tunnel ionization by the laser electric field $\mathbf{E}$, $\omega_{pm}^2 = 4\pi n_m e^2/m$, where n_m is the initial density of neutral atoms, $E_A = (4/3)(2m)^{1/2} I_0^{3/2}/e\hbar$ is the characteristic atomic field, I_0 is the ionization potential and $h = 2\pi\hbar$ is the Plank's constant. Equation (2) is written in the limit when $mv_0^2/2 \gg I_0$, where $v_0 = e|\mathbf{E}|/m\omega$; $mv_0^2/2 \gg 1500 P_{16}\lambda_\mu^2$ in eV, P_{16} is laser power density in units of 10^{16} W/cm^2 and λ_μ is the laser wavelength in microns. Inside the ionizing gas $(z > z_g)$,

$$\mathbf{E} = \hat{x}A(t,z,r)\cos(\omega t - \omega z/c)\exp[-(t-(z-z_L)/v_g)^2/\tau_L^2],$$

where $v_g = c(1-\omega_{p0}^2/\omega^2)^{1/2}$ is the group velocity of laser pulse, $\omega_{p0}^2 = \omega_p^2(t,z,r=0)$.

The wave equation for the laser pulse is

$$\nabla^2\mathbf{E} - \frac{1}{c^2}\frac{\partial^2\mathbf{E}}{\partial t^2} = \frac{\omega_p^2}{c^2}\mathbf{E}. \quad (4)$$

Substituting for $\mathbf{E}$, we obtain, to successive orders in the WKB approximation,

$$2ik\frac{\partial A}{\partial z} + \frac{2i\omega}{c^2}\frac{\partial A}{\partial t} + \nabla_\perp^2 A = \frac{A}{c^2}[\omega_p^2(t,z,r) - \omega_{p0}^2(t,z)], \quad (5)$$

defining $t' = t - z/c$ and assuming $\omega_p^2/\omega^2 \ll 1$; we can rewrite the above equation as

$$\frac{2i\omega}{c}\frac{\partial A}{\partial z} + \nabla_\perp^2 A = \frac{\omega_p^2 - \omega_{p0}^2}{c^2}. \quad (6)$$

We consider cylindrically symmetric propagation and write $A = A_0 \exp(iS)$, where $A_0(t',z,r)$ and $S(t',z,r)$ are real. Separating real and imaginary parts of Eq. (6), we obtain

$$-\frac{2\omega}{c}\frac{\partial S}{\partial z}A_0 + \frac{\partial^2 A_0}{\partial r^2} + \frac{1}{r}\frac{\partial A_0}{\partial r} - \left(\frac{\partial S}{\partial r}\right)^2 A_0 = \frac{\omega_p^2 - \omega_{p0}^2}{c^2}A_0, \quad (7)$$

$$\frac{\omega}{c}\frac{\partial A_0^2}{\partial z} + \left(\frac{\partial^2 S}{\partial r^2} + \frac{1}{r}\frac{\partial S}{\partial r}\right)A_0^2 + \frac{\partial S}{\partial r}\frac{\partial A_0^2}{\partial r} = 0. \quad (8)$$

The above equations can be solved by expanding ω_p^2 and S in powers of r^2. In the usual near-axis approximation one expands ω_p^2 and S, only to the first power in r^2, i.e., $\omega_p^2 = \omega_{p0}^2 + \omega_{p2}^2 r^2/r_0^2$ and $S = S_0 + S_2 r^2/r_0^2$, then Eq. (8) can be integrated to give

$$A_0 = \frac{E_0}{f}\exp(-r^2/2r_0^2 f^2), \quad (9)$$

where $f(z,t')$ is the beam width parameter.

In the following discussion we will use the dimensionless variables $\omega_{p0}^2 \to \omega_{p0}^2/\omega^2$, $\omega_{p2}^2 \to \omega_{p2}^2/\omega^2$, $\omega_{pm}^2 \to \omega_{pm}^2/\omega^2$, $t' \to \omega t'$, $t \to \omega t$, $\tau_L \to \omega\tau_L$, $x \to \omega x/c$, $z \to \omega z/c$, $z_L \to \omega z_L/c$, $z_g \to \omega z_g/c$, $r_0 \to \omega r_0/c$, $r \to \omega r/c$, $p_x \to p_x/m_0 c$, $p_z \to p_z/m_0 c$, $a_0 \to eE_0/m_0\omega c$. The equations governing defocusing are

$$\frac{\partial \omega_{p0}^2}{\partial t'} = (\omega_{pm}^2 - \omega_{p0}^2)\frac{I_0}{\hbar\omega}\left(\frac{\pi E_0}{2E_A f}\right)^{1/2}\exp\left[-\frac{E_A}{E_0}f\right], \quad (10)$$

$$\frac{\partial \omega_{p2}^2}{\partial t'} = \left(-\omega_{p2}^2 - (\omega_{pm}^2 - \omega_{p0}^2)\frac{E_A}{2E_{00}f}\right)\frac{I_0}{\hbar\omega}\left(\frac{\pi E_0}{2E_A f}\right)^{1/2} \times \exp\left[-\frac{E_A}{E_0}f\right], \quad (11)$$

$$r_0^2\frac{\partial^2 f}{\partial z^2} = \frac{1}{r_0^2 f^3} - \frac{\omega_{p2}^2 f}{\omega^2}. \quad (12)$$

The equations governing electron momentum and energy are

$$\frac{dP_x}{dt} = -\frac{a_0}{f}\exp\left[-\frac{(t-(z-z_L)/(1-\omega_{p0}^2/\omega^2)^{1/2})^2}{\tau_L^2}\right] \times \exp\left[-\frac{r^2}{2r_0^2 f^2}\right]\left(1 - \frac{p_z}{\gamma}\right)\cos(t-z), \quad (13)$$

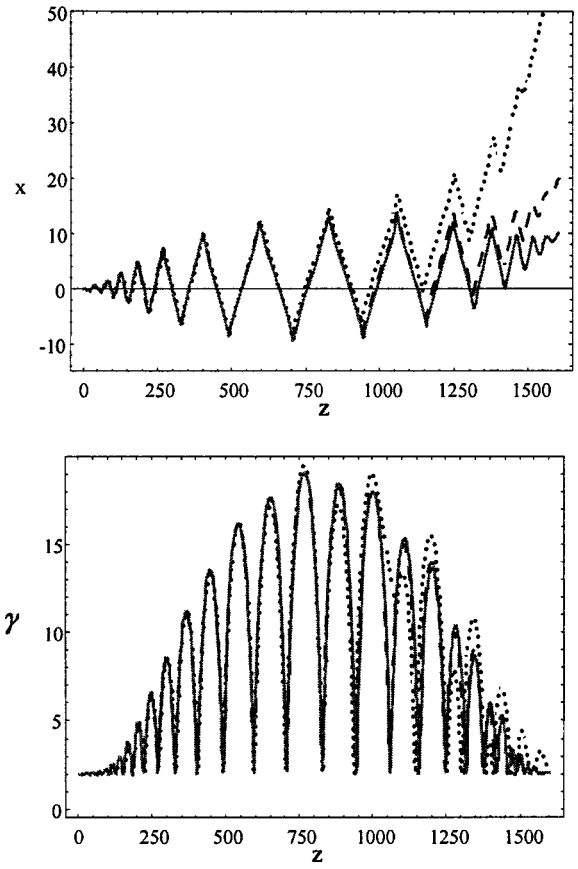

FIG. 2. (a) Electron trajectories in the x-z plane and (b) electron energy γ as a function of z for $a_0=3$, $\gamma_0=2$, and $r_0=75$, 110, and 150 (dotted, dashed, and solid lines, respectively) in vacuum.

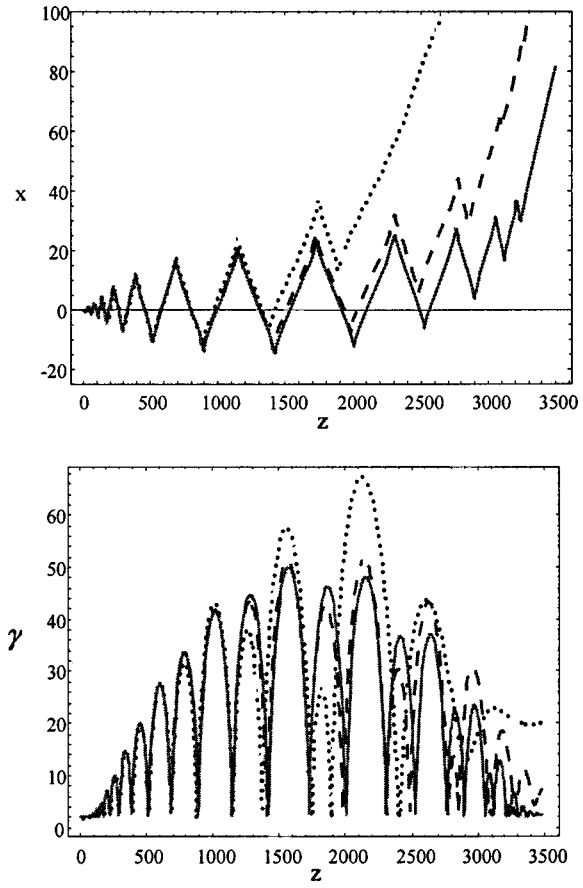

FIG. 3. (a) Electron trajectories in the x-z plane and (b) electron energy γ as a function of z for $a_0=5$, $\gamma_0=2$, and $r_0=75,110$, and 150 (dotted, dashed, and solid lines, respectively) in vacuum.

$$\frac{dP_z}{dt} = -\frac{a_0}{f}\exp\left[-\frac{(t-(z-z_L)/(1-\omega_{p0}^2/\omega^2)^{1/2})^2}{\tau_L^2}\right] \times\exp\left[-\frac{r^2}{2r_0^2f^2}\right]\frac{p_x}{\gamma}\cos(t-z), \tag{14}$$

$$\frac{d\gamma}{dt} = -\frac{a_0}{f}\exp\left[-\frac{(t-(z-z_L)/(1-\omega_{p0}^2/\omega^2)^{1/2})^2}{\tau_L^2}\right] \times\exp\left[-\frac{r^2}{2r_0^2f^2}\right]\frac{p_x}{\gamma}\cos(t-z). \tag{15}$$

Equations (10)–(15) are ordinary differential equations. We have solved them numerically by fourth order Runge-Kutta method by taking position of the electron as a function of time, with $\mathbf{r}=0$, $P_x=0$, $\gamma=2$, $\omega_{p0}=0$, $\omega_{p2}=0$, $\partial f/\partial t=0$, and $f=1$ at $t=0$. We have obtained electron trajectories in the x-z plane, the energy γ, and the beam width parameter as a function of z for different parameters. Our results are as follows.

III. NUMERICAL RESULTS

We choose following parameters: $\tau_L=25$, $z_L=-50$, $I_0=21$ eV, $E_A/E_0=3$ (corresponding to singly ionized helium gas), and $\lambda=2\pi c/\omega=1$ μm. Point z_g has been chosen around the point at which the peak of the pulse interacts with the electron, so that the pulse interacts with the electron in a gas during the trailing part.

Figures 2 and 3 show electron trajectories in the x-z plane and energy γ as a function of z at $a_0=3$ and 5, respectively, for different laser spot sizes $r_0=75,110$, and 150 in vacuum (no gas). The electron gains energy during the rising part of the laser pulse and losses it during the trailing part, resulting in negligible net energy gain in Fig. 2 and for $r_0=150$ in Fig. 3. However, for a high laser intensity and small spot size, an electron may escape from the laser pulse and can retain a small energy, as can be seen from the Fig. 3.

Figures 4 and 5 show the electron energy γ and beam width parameter f as functions of z at $a_0=3$ for $r_0=75$ and 150, respectively. The initial densities of the neutral gas atoms are $\omega_{pm}^2=0.08$, 0.1, and 0.12 and $\omega_{pm}^2=0.1$, 0.13, and 0.2, respectively. The laser pulse defocuses during the trailing part of the pulse and the electron gains net energy. Higher gas density results in higher defocusing and electron retains more energy. It can be seen that initial density of the neutral gas atoms required to defocus the laser pulse increases with laser spot size.

Figures 6 and 7 show the electron energy γ and beam width parameter f as functions of z at $a_0=5$ for $r_0=75$ and 150, respectively. The initial densities of the neutral gas atoms are $\omega_{pm}^2=0.03$, 0.04, and 0.05 and $\omega_{pm}^2=0.045$, 0.06,

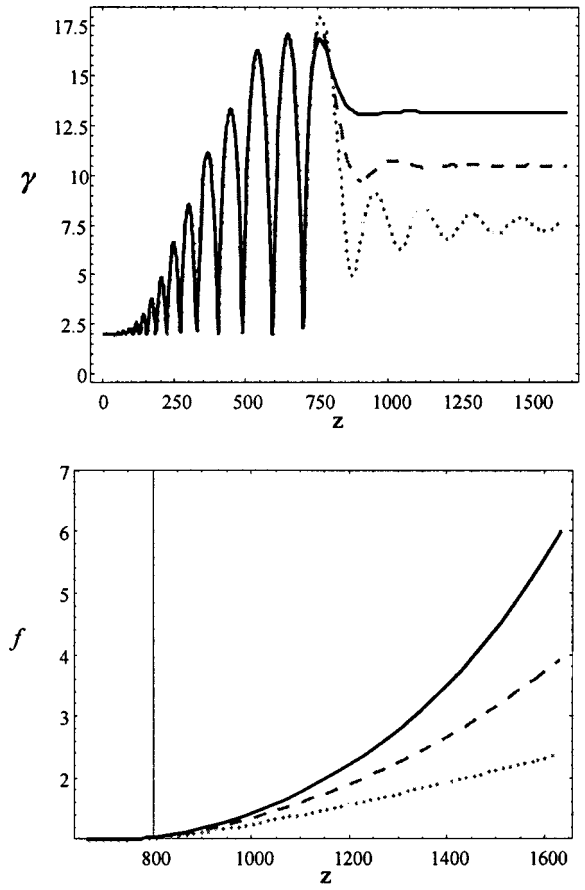

FIG. 4. (a) Electron energy γ and (b) beam width parameter f as a function of z for $a_0=3$, $\gamma_0=2$, $r_0=75$, $z_g=710$, and $\omega_{pm}^2=0.08$, 0.1, and 0.12 (dotted, dashed, and solid lines, respectively).

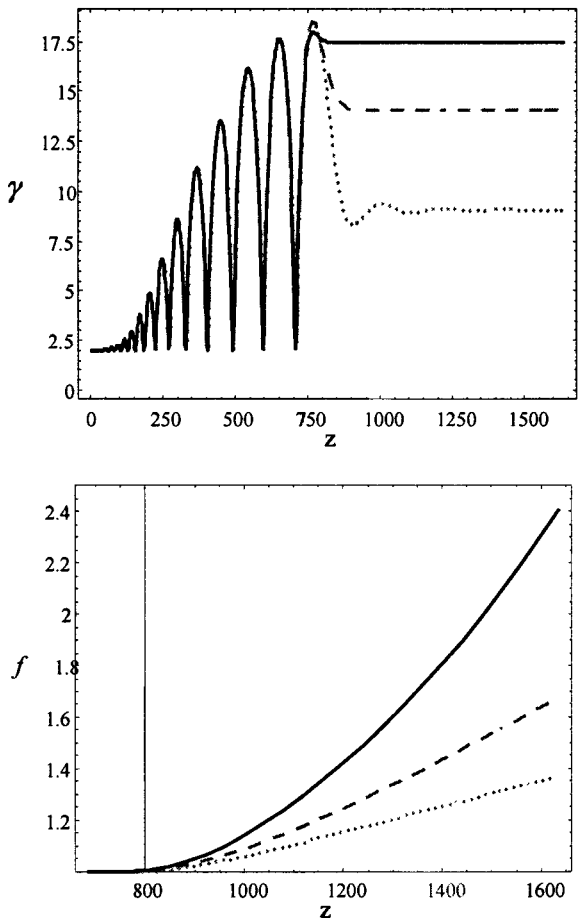

FIG. 5. (a) Electron energy γ and (b) beam width parameter f as a function of z for $a_0=3$, $\gamma_0=2$, $r_0=150$, $z_g=730$, and $\omega_{pm}^2=0.1$, 0.13, and 0.2 (dotted, dashed, and solid lines, respectively).

and 0.075, respectively. The higher gas density results in a higher defocusing, and the electron retains more energy, and the initial density of the neutral gas atoms required to sufficiently defocus the laser pulse increases with the laser spot size; these are the same results as in Figs. 4 and 5. The electron gains more energy, and gas density required to defocus the laser pulse is lower than that in the corresponding cases at lower laser intensity; see Figs. 4 and 5.

From the results we can conclude that an electron cannot gain net energy if laser spot size is large and the laser intensity is low. However, for a small spot size and high laser intensity, an electron can escape from the laser pulse and can gain some net energy. The electron can always retain the energy gained by it, if a gas of sufficient density is used to defocus the laser pulse during the trailing part of the laser pulse. The defocusing increases with an increase in the laser intensity and the initial density of neutral gas atoms and with a decrease in the spot size of the laser pulse. If a laser pulse is properly defocused, an electron retains more energy.

IV. DISCUSSION

An electron gains energy during the rising part of the laser pulse and loses it during the trailing part. However, if laser intensity is high and the spot size is small, an electron can escape from the field of the pulse and can retain some energy. If a gas is used to defocus the laser pulse during the trailing part of the pulse, an electron experiences the action of ponderomotive deceleration at the trailing part of the pulse with a lower intensity as compared to acceleration at the rising part, and thus gains net energy. The initial density of neutral gas atoms should be high enough to properly defocus the laser pulse; otherwise the electron experiences some deceleration during the trailing part of the pulse and the net energy gain reduces. A high laser intensity or a small laser spot size causes a higher rate of tunnel ionization and a higher defocusing of the laser pulse; therefore the required initial density of neutral gas atoms decreases with the increase in the laser intensity and with the decrease in laser spot size. If the gas starts before or after the point at which the peak of the pulse interacts with electron, the net energy gained by the electron reduces. This can be understood as follows: if the gas starts during the rising part of the laser pulse the peak intensity experienced by the electron decreases, and if the gas starts during the trailing part the electron loses some energy interacting with this part. Experimentally, for some electrons gas will not start from a point where the peak of the pulse interacts with electron, therefore, elec-

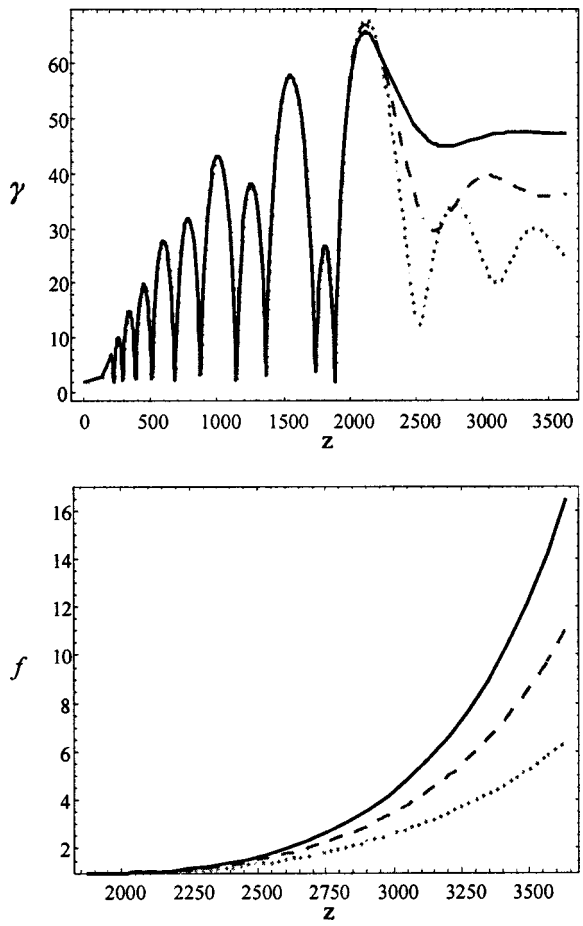

FIG. 6. (a) Electron energy γ and (b) beam width parameter f as a function of z for $a_0=5$, $\gamma_0=2$, $r_0=75$, $z_g=1925$, and $\omega_{pm}^2=0.03$, 0.04, and 0.05 (dotted, dashed, and solid lines, respectively).

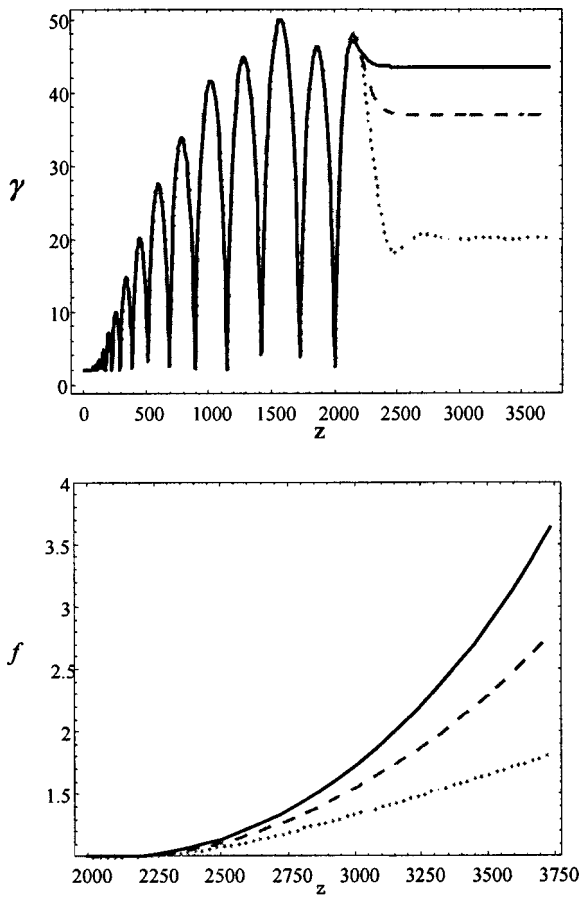

FIG. 7. (a) Electron energy γ and (b) beam width parameter f as a function of z for $a_0=3$, $\gamma_0=2$, $r_0=150$, $z_g=2050$, and $\omega_{pm}^2=0.045$, 0.06, and 0.075 (dotted, dashed, and solid lines, respectively).

trons with a range of energies will be obtained in this scheme.

We have chosen the radial and temporal intensity profiles to be Gaussian both in vacuum and gas for the sake of simplicity. However, actual profiles may be different in the gas. If the fall in intensity is sharper, then the required values of the initial density of the neutral gas atoms will be lower than that reported in this paper, and vice versa; however, the suggested scheme will remain equally effective.

ACKNOWLEDGEMENT

One of the authors (K.P.S.) is grateful to CSIR, Government of India, for financial support.

[1] A. Modena *et al.*, Nature (London) **377**, 606 (1995).
[2] M. I. K. Santala *et al.*, Phys. Rev. Lett. **84**, 1459 (2000).
[3] M. D. Perry *et al.*, Opt. Lett. **24**, 1459 (2000).
[4] D. Umstadter, Phys. Plasmas **8**, 1774 (2001); J. Phys. D **36**, R151 (2003), and references therein.
[5] E. Esarey, P. Sprangle, J. Krall, and A. Ting, IEEE Trans. Plasma Sci. **24**, 252 (1996), and references therein.
[6] P. Chen, Part. Accel. **20**, 171 (1985).
[7] T. Tajima and J. M. Dawson, Phys. Rev. Lett. **43**, 267 (1979).
[8] L. M. Gorbunov and V. I. Kirsanov, Zh. Eksp. Teor. Fiz. **93**, 509 (1987) [Sov. Phys. JETP **66**, 290 (1987)].
[9] D. Umstadter, E. Esarey, and J. K. Kim, Phys. Rev. Lett. **72**, 1224 (1994).
[10] P. Sprangle, E. Esarey, J. Krall, and G. Joyce, Phys. Rev. Lett. **69**, 2200 (1992).
[11] T. M. Antonsen, Jr. and P. Mora, Phys. Rev. Lett. **69**, 2204 (1992).
[12] N. E. Andreev, L. M. Gorbunov, V. I. Kirsanov, A. Pogosova, and R. R. Ramazashvili, Pis'ma Zh. Eksp. Teor. Fiz. **55**, 551 (1992) [JETP Lett. **55**, 571 (1992)].
[13] C. L. Moore, A. Ting, T. Jones, E. Briscoe, B. Hafizi, R. F. Hubbard, and P. Sprangle, Phys. Plasmas **8**, 2481 (2001).
[14] C. Gahn, G. D. Tsakiris, G. Pretzler, K. J. Witte, P. Thirolf, C. Delfin, and C.-G Wahlstrom, Phys. Plasmas **9**, 987 (2002).
[15] A. V. Soldatov, Plasma Phys. Rep. **27**, 153 (2001).
[16] Wei Yu, V. Bychenkov, Y. Sentoku, M. Y. Yu, Z. M. Sheng,

and K. Mima, Phys. Rev. Lett. **85**, 570 (2000).
[17] X. Wang, M. Krishnan, N. Saleh, H. Wang, and D. Umstadter, Phys. Rev. Lett. **84**, 5324 (2000).
[18] S. A. Akhmanov, A. P. Sukhorukov, and R. V. Khokhlov, Usp. Fiz. Navk **93**, 19 (1967) [Sov. Phys. Usp. **10**, 609 (1968)].
[19] E. Esarey, P. Sprangle, J. Krall, and A. Ting, IEEE J. Quantum Electron. **33**, 1879 (1997), and references therein.
[20] C. S. Liu and V. K. Tripathi, Phys. Plasmas **7**, 4360 (2000).
[21] D. N. Gupta and A. K. Sharma, Phys. Scr. **67**, 246 (2003).